

# Experimental device-independent certified randomness generation with an instrumental causal structure

Iris Agresti,<sup>1</sup> Davide Poderini,<sup>1</sup> Leonardo Guerini,<sup>2</sup> Michele Mancusi,<sup>1</sup> Gonzalo Carvacho,<sup>1</sup> Leandro Aolita,<sup>2,3</sup> Daniel Cavalcanti,<sup>4</sup> Rafael Chaves,<sup>5,6</sup> and Fabio Sciarrino<sup>1</sup>

<sup>1</sup>*Dipartimento di Fisica, Sapienza Università di Roma, Piazzale Aldo Moro 5, I-00185 Roma, Italy*

<sup>2</sup>*International Center of Theoretical Physics - South American Institute for Fundamental Research, Instituto de Física Teórica - UNESP, R. Dr. Bento T. Ferraz 271, 01140-070, São Paulo, Brazil*

<sup>3</sup>*Instituto de Física, Universidade Federal do Rio de Janeiro, Caixa Postal 68528, Rio de Janeiro, RJ 21941-972, Brazil*

<sup>4</sup>*ICFO - Institut de Ciències Fotoniques, The Barcelona Institute of Science and Technology, E-08860 Castelldefels, Barcelona, Spain*

<sup>5</sup>*International Institute of Physics, Federal University of Rio Grande do Norte, 59078-970, P. O. Box 1613, Natal, Brazil*

<sup>6</sup>*School of Science and Technology, Federal University of Rio Grande do Norte, 59078-970 Natal, Brazil*

The generation of random numbers is a central challenge for a plethora of fields, ranging from scientific numerical simulations, cryptography and randomized computations to safeguarding privacy and gambling. The intrinsic random nature of quantum physics offers novel tools for this aim. Bell non-local correlations obtained by measurements on entangled states allow for the generation of bit strings whose randomness is guaranteed in a device-independent manner, i.e. without assumptions on the measurement and state-generation devices. Here, we generate this strong form of certified randomness on a new platform: the so-called instrumental scenario, which is central to the field of causal inference. First, we demonstrate that the techniques previously developed for the Bell scenario can be adapted to the instrumental process. As the following step, we experimentally realize a quantum instrumental process using entangled photons and active feed-forward of information, implementing a device-independent certified-randomness generation protocol, producing 28273 certified random bits, with a maximum extracted certified bits rate of 0.38 Hz. This work constitutes a proof-of-principle of the quantum instrumental causal network as a practical resource for information processing tasks, offering a valuable alternative to Bell-like scenarios.

## INTRODUCTION

The generation of random numbers has applications in a wide range of fields, from scientific research – e.g. to simulate physical systems – to military scopes – e.g. for effective cryptographic protocols – and every-day concerns – like ensuring privacy and gambling. From a classical point of view, the concept of randomness is tightly bound to the incomplete knowledge of a system; indeed, classical randomness has a subjective and epistemological nature and is erased when the system is completely known [1]. Hence, classical algorithms can only generate pseudo-random numbers [2], whose unpredictability relies on the complexity of the device generating them. Besides, the certification of randomness is an elusive task, since the available tests can only verify the absence of specific patterns, which may go undetected but still be known to an adversary [3].

On the other hand, randomness is intrinsic to quantum systems, which do not possess definite properties until these are measured. In real experiments, however, this intrinsic quantum randomness comes embedded with noise and lack of complete control over the device, compromising the security of quantum random-number generation. A solution to that is to devise quantum protocols whose correctness can be certified in a device-independent (DI) manner, i.e. solely from the observed statistics and with no assumption whatsoever on the internal working of the experimental devices [4]. For instance, only from the extent of the observed CHSH inequality violation [5], one can put a lower bound on the certified randomness characterizing the measurement outputs of the two

parties performing the Bell test. After the seminal work [4], several protocols of *randomness amplification*, i.e. to generate near-perfect randomness, from a source of weak randomness, and *quantum key distribution*, i.e. sharing a common secret string through communication over public channels, have been developed exploiting Bell inequalities [6–18]. In particular, loophole-free Bell tests based randomness generation protocol have been implemented [4, 16, 19] and more advanced techniques have been developed to provide security against general adversarial attacks in [17].

From a causal perspective, the non-classical behaviour revealed by a Bell test lies in the incompatibility of quantum predictions with our intuitive notion of cause and effect [20–22]. Given that the causal structure underlying a Bell-like scenario involves five variables (the measurement choices and outcomes for each of the two observers and a fifth variable representing their shared correlations), it is natural to wonder whether a simpler causal structure could give rise to an analogous discrepancy between quantum and classical causal predictions [23]. Indeed, as reported for the first time in [24], the simplest scenario, in terms of involved nodes' number, achieving this result is the instrumental causal structure [25, 26] (shown in Fig. 1-a), where the two parties (A and B) are linked by a classical channel of communication. This scenario has fundamental importance in causal inference, since it allows the estimation of causal influences even in the presence of unknown latent factors [25].

In this letter, we provide a proof-of-principle that the instrumental scenario can be exploited to devise a DI randomness generation and certification protocol. Indeed, we show

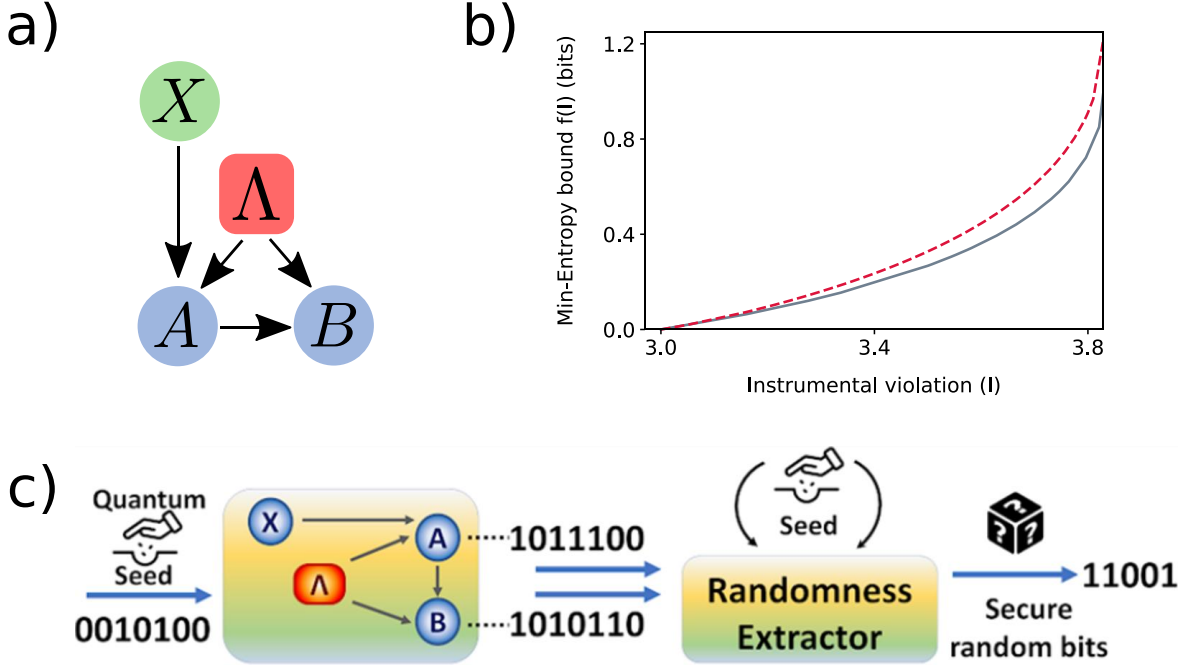


FIG. 1. **Randomness generation and certification protocol.** **a)** Instrumental causal structure represented as a directed acyclic graph [22] (DAG), where each node represents a variable and the arrows link variables between which there is causal influence. In this case,  $X$ ,  $A$  and  $B$  are observable, while  $\Lambda$  is a latent variable. **b)** The main plot shows the lower bounds  $f_x(\mathcal{I})$  to  $H_\infty(A, B|E, x)$  as a function of  $\mathcal{I}$ , for inputs  $x = 1$  (grey) and  $x = 2, 3$  (dashed red). Interestingly, unlike what happens in CHSH scenario [4, 18], there is a difference in the bounds corresponding to different inputs, indeed the certified randomness for  $x = 1$  is slightly smaller than that for  $x = 2, 3$ . **c)** The randomness generation and certification protocol is made up of three stages: (i) initial seed generation (defining Alice’s choice between the operators), (ii) instrumental process implementation, (iii) classical randomness extractor. The initial seed is obtained from the random bits provided by the NIST Randomness Beacon [37]. In the second stage, Alice’s and Bob’s outputs are collected and characterized by the min-entropy corresponding to the value of the instrumental violation  $\mathcal{I}^*$ , according to the relation shown in Fig.1-b. The value of the min-entropy indicates the number of certified random bits that can be extracted. At the end, those strings are injected in a classical randomness extractor (Trevisan’s extractor [27]) and the certified random bits are extracted. The extractor’s seed is as well provided by the NIST Randomness Beacon.

for the first time that the sequence of the measurement outputs obtained by the parties within an instrumental process is characterized by a minimum amount of randomness, quantified by the min-entropy of the bit-string, which depends and is certified by the observed instrumental violation. Therefore, we demonstrate that the techniques previously developed for the Bell scenario can be adapted to the instrumental process venue, offering a valid alternative platform which involves a causal structure requiring less number of inputs than the Bell scenario. To implement the protocol in all of its parts, we have setup a classical extractor following the theoretical design by Trevisan [27]. This work opens the way to other applications of the instrumental scenario in the field of device independent protocols, which until now have relied primarily on Bell-like tests.

## RANDOMNESS CERTIFICATION VIA INSTRUMENTAL INEQUALITY VIOLATIONS

Let us first briefly review the previous results obtained within the Bell inequalities context [28]. In a CHSH (Clauser Horne Shimony Holt) scenario [5], two parties,  $A$  and  $B$ , share a bipartite system and, without communicating to each other, perform local measurements on their subsystem. If  $A$  and  $B$  choose between two given operators each, i.e.  $(A_1, A_2)$  and  $(B_1, B_2)$  respectively, and then combine their data, the mean value of the operator  $S = |\langle A_1, B_1 \rangle - \langle A_1, B_2 \rangle + \langle A_2, B_1 \rangle + \langle A_2, B_2 \rangle|$  should be upper-bounded by 2, for any deterministic model respecting a natural notion of locality. However, as proved in [5], if  $A$  and  $B$  share an entangled state, they can get a value exceeding such bound, whose explanation requires the presence of non-classical correlations between the two parties. Hence, Bell inequalities have been adopted in [4] to guarantee the intrinsic random nature of the measurements’ outcomes, within a DI randomness generation and certification protocol.

In the instrumental scenario, which can be depicted with the causal structure in Fig.1-a, two parties (Alice and Bob) share a bipartite state. Alice can choose among  $m$  possible  $d$ -outcome measurements ( $O_A^1, \dots, O_A^m$ ), according to the *instrument* variable  $X$ , which can assume  $m$  different values, while Bob's choice among  $d$  observables ( $O_B^1, \dots, O_B^d$ ) depends on Alice's outcome. In other words, as opposed to the spatial correlations in a Bell-like scenario, the instrumental process constitutes a temporal scenario, with one-way communication of Alice outcomes to select Bob's measurement. In analogy with Bell-like scenarios, the causal structure underlying an instrumental process imposes some constraints on the classical joint probabilities  $P(a, b|x)$  that are compatible with it [25, 26] (the so-called instrumental inequalities) and, as shown in [24], those inequalities can be violated when Alice and Bob perform their measurements on entangled states. In the particular case where the instrument  $X$  can assume three different values (1,2,3), while  $a$  and  $b$  are dichotomic, the following inequality holds [26]:

$$\mathcal{I} = \langle A \rangle_1 - \langle B \rangle_1 + 2 \langle B \rangle_2 - \langle AB \rangle_1 + 2 \langle AB \rangle_3 \leq 3 \quad (1)$$

where  $\langle AB \rangle_x = \sum_{a,b=0,1} (-1)^{a+b} P(a, b|x)$ . Remarkably, this inequality can be violated with the correlations produced by quantum instrumental causal models [24]. The maximal value attained by such quantum models is  $\mathcal{I} = 1 + 2\sqrt{2}$ . Recently the relationship with the Bell scenario has been studied in [29].

In this context, we show that if a given statistics  $P(a, b|x)$  violates inequality (1), then private random bits can be extracted from their measurement outcomes. More precisely, we consider the general scenario where, in addition to Alice and Bob, there exists a third observer – an adversary eavesdropper Eve – who tries to guess Alice and Bob's outcomes. That is, Eve has some (classical) side information  $e$ , which may be correlated with  $(a, b)$ . For instance, the quantum state from which Alice and Bob obtain  $a$  and  $b$  could actually be part of a tripartite state shared with Eve and  $e$  could then be the outcome of a measurement on her share of the state. For a given input  $x$ , the correlations between  $(a, b)$  and  $e$  are given by an extended joint distribution  $P(a, b, e|x)$  that marginalizes to the observed statistics, i.e.  $\sum_e P(a, b, e|x) = P(a, b|x)$ . For each  $x$ , the randomness of  $(a, b)$  with respect to  $e$  can be quantified by the conditional min-entropy  $H_\infty(A, B|E, x) = -\log_2[\sum_e P(e) \max_{a,b} P(a, b|e, x)]$  [30]. Interestingly, the quantity inside the logarithm gives the optimal guessing probability by Eve, i.e., the probability that  $e = (a, b)$ , for each  $x$ , over all possible guessing strategies and average over her side information  $e$ :  $P_{\text{guess}}(x) = \sum_e P(e) \max_{a,b} P(a, b|e, x)$ . This is due to the fact that Eve's optimal guessing strategy is known to consist of simply betting for the most likely outcome given her side information  $e$  and  $x$  [31, 32]. Thus,  $H_\infty(A, B|E, x) = -\log_2[P_{\text{guess}}(x)]$ .

Now, the fact that  $P(a, b|x)$  violates Eq. (1) imposes non-trivial constraints on its possible extensions  $P(a, b, e|x)$ . In particular, it restricts the values  $H_\infty(A, B|E, x)$  can take. Indeed, it is possible to obtain a lower-bound

on  $H_\infty(A, B|E, x)$ , for each  $x$ , as a function  $f_x$  of  $\mathcal{I}$ :  $H_\infty(A, B|E, x) \geq f_x(\mathcal{I})$ . For each  $x$  and  $\mathcal{I}$ , the lower bound  $f_x(\mathcal{I})$  can be computed by applying to the instrumental case the numerical techniques developed in [34] originally for the Bell scenario (see Methods), via semidefinite programming (SDP). The functions  $f_x$  are convex and grow monotonically with  $\mathcal{I}$ ; so that the higher the violation of Eq. (1) is, the higher the min-entropy. Hence, the violation can certify both the randomness of the outcomes as well as their privacy with respect to any adversary. In Fig. 1-b, we plot  $f_x(\mathcal{I})$  as a function of  $\mathcal{I}$  for all three values of  $x$ . Interestingly, the certified randomness for  $x = 1$  is slightly smaller than that for  $x = 2, 3$ .

The entropy bounds obtained above require one to know  $\mathcal{I}$ . However, in actual implementations, the exact distribution is unknown and one can only get a finite-sample estimate  $\mathcal{I}^*$  of  $\mathcal{I}$ . To account for this, we adapt the finite-sample statistical analysis developed in Ref. [4] for the Bell case to our instrumental scenario. More precisely, we consider  $n$  experimental runs, with inputs given by a string  $\mathbf{s} = (x_1, \dots, x_n)$ , which produce a  $2n$ -long output string  $\mathbf{r} = (a_1, b_1, \dots, a_n, b_n)$ . The estimate  $\mathcal{I}^*$  is defined as  $\mathcal{I}$  in Eq. (1) but with the actual expectation values substituted by finite-sample averages over the  $n$  runs. The private randomness of the  $2n$ -bit output string  $\mathbf{r}$ , given the input string  $\mathbf{s}$ , is quantified by the min-entropy  $H_\infty(\mathbf{R}|E, \mathbf{s})$ , defined analogously to  $H_\infty(A, B|E, x)$  but with  $\mathbf{r}$  and  $\mathbf{s}$  instead  $(a, b)$  and  $x$ , respectively. A lower-bound of the following form on  $H_\infty(\mathbf{R}|E, \mathbf{s})$  as a function of  $\mathcal{I}^*$  can be obtained adapting the strategy in [4] to the instrumental case, which is done simply setting, on each run,  $y = a$ :

$$H_\infty(\mathbf{R}|E, \mathbf{s}) \geq n f_1(\mathcal{I}^* - \gamma), \quad (2)$$

with probability at least  $1 - \delta$ , where  $\gamma = \sqrt{-2 \log \delta / n} \frac{1}{q} + |\mathcal{I}_q|$  is the statistical error of the estimation, which depends on the finite size of the sample ( $n$ ), on the probability  $q$  of the least probable input ( $x$ ), on  $\delta$  and on the maximum achievable quantum violation  $\mathcal{I}_q$ , which in our case amounts to  $1 + 2\sqrt{2}$ . Note that, for any fixed  $q$  and desired failure probability  $\delta$ ,  $\gamma$  can be made arbitrarily small by increasing the sample size  $n$ . The failure probability  $\delta$  comes to play, in order not to make the *iid* assumption on the adopted device (for further details see Appendix A.2 of [4], whose calculations, originally made for Bell-like scenarios, hold also in the case of the Instrumental scenario). This bound gives the minimum number of certified random bits that can be extracted from the obtained  $2n$ -bit raw output by a classical randomness-extraction algorithm, in order to obtain a certified random bits string. We feed our raw string to use our implementation of the extractor theoretically devised by Trevisan [27] (our code can be found at [36]). The extraction protocol outputs at most  $n f_1(\mathcal{I}^* - \gamma)$  certified random bits, according to a parameter  $\epsilon$  set by the user as a preliminary, in our case  $10^{-7}$  (for further details about the randomness extractor, see the Supplementary Material). Summarizing, the proposed certified random number generation protocol consists of implementing a quantum instrumental process, where the input  $x$  is given at each experimental run by the NIST randomness Beacon, then collecting the  $2n$

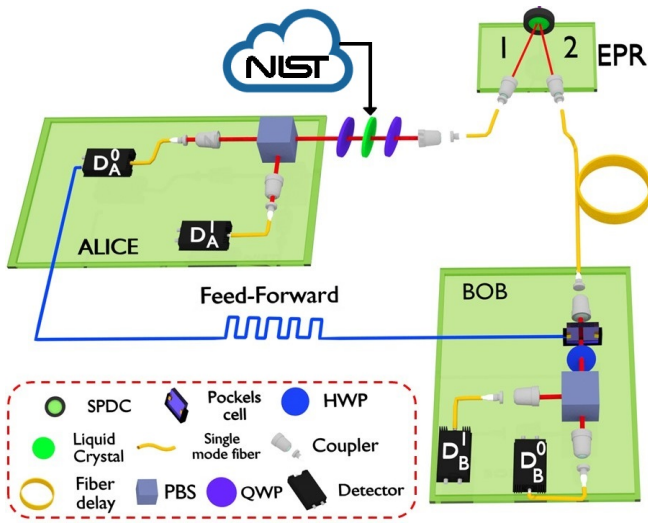


FIG. 2. **Experimental apparatus:** A polarization-entangled photon pair is generated via spontaneous parametric down-conversion (SPDC) process in a nonlinear crystal. Photon 1 is sent to the Alice’s station, where one of three observables ( $O_A^1$ ,  $O_A^2$  and  $O_A^3$ ) is measured through a liquid crystal followed by a polarizing beam splitter (PBS). Detector  $D_A^0$  acts as trigger for the application of a 1280 V voltage on the Pockels cell, whenever the measurement output 0 is registered. The photon 2 is delayed 600 ns before arriving to Bob’s station by employing a single-mode fiber 125 m long. After leaving the fiber the photon passes through the Pockels cell, followed by a fixed HWP at  $56.25^\circ$  and a PBS. If the Pockels cell has been triggered (in case of A measurement outcome is 0), its action combined to the fixed HWP in Bob’s station allows us to project onto  $O_B^1$ . Otherwise (if A measurement outcome is 1), the Pockels cell acts as the identity and we project onto  $O_B^2$ .

output bits, evaluating the corresponding experimental value of  $\mathcal{I}^*$  and setting the desired value of the security parameter  $\delta$ , in our case to 0.01. At this point, the minimum number of certified random bits that can be extracted is  $n^* f(\mathcal{I}^* - \gamma)$ , where  $\gamma$  depends on  $\delta$ ,  $n$  and  $q$ , that, considering equiprobable inputs, is  $1/3$ . Finally, these bits are extracted with Trevisan’s extraction protocol and constitute the final output of our protocol.

### EXPERIMENTAL IMPLEMENTATION OF THE PROTOCOL

The device-independent random numbers generator, in our proposal, is made up of three main parts, which are seen as black boxes to the user: the state generation and Alice’s and Bob’s measurement stations. The causal correlations among these three stages are those of an instrumental scenario (see Fig. 1-a-c) and are implemented through the photonic platform depicted in Fig.2.

Within this experimental apparatus, the qubits are encoded in the photon’s polarization: horizontal ( $|H\rangle$ ) and vertical ( $|V\rangle$ ) polarizations represent, respectively, qubits  $|0\rangle$  and  $|1\rangle$ , eigenstates of the Pauli matrix  $\sigma_z$ . A spontaneous parametric

down-conversion (SPDC) process generates the two-photon maximally entangled state  $|\Psi^-\rangle = \frac{|HV\rangle - |VH\rangle}{\sqrt{2}}$ . One photon is sent to path 1, towards Alice’s station, where an observable among  $O_A^1$ ,  $O_A^2$  and  $O_A^3$  is measured, applying the proper voltage to a liquid crystal (LCD). The voltage must be chosen according to a random seed, made of a string of trits. This seed is obtained from the NIST Randomness Beacon [37], which provides 512 random bits per minute. After Alice has performed her measurement, whenever she gets output 1 (i.e.  $D_A^0$  registers an event), the detector’s signal is split to reach the coincidence counter and, at the same time, trigger the Pockels cell on path 2. Bob’s station is made of a Half-Wave Plate (HWP) followed by this fast electro-optical device. When no voltage is applied to the Pockels cell, Bob’s operator is  $O_B^1$  and, when it is turned on, there is a swift changes to  $O_B^2$  (the cell’s time response is of the order of nanoseconds). In order to have the time to register Alice’s output and select Bob’s operator accordingly, the photon on path 2 is delayed, through a 125 meters long single-mode fiber.

The four detectors are synchronized in order to distinguish the coincidence counts generated by the entangled photons’ pairs from the accidental counts. The measurement operators achieving maximal violation of  $\mathcal{I} = 1 + 2\sqrt{2}$ , when applied to the state  $|\psi^-\rangle$ , are the following:  $O_A^1 = -(\sigma_z - \sigma_x)/\sqrt{2}$ ,  $O_A^2 = -\sigma_x$ ,  $O_A^3 = \sigma_z$  and  $O_B^1 = (\sigma_x - \sigma_z)/\sqrt{2}$ ,  $O_B^2 = -(\sigma_x + \sigma_z)/\sqrt{2}$ . After having implemented the instrumental scenario, collected the raw bits characterized by a violation of the instrumental inequality and by its corresponding min-entropy, we executed the classical randomness extractor devised by Trevisan [27] and adopted also in [33]. Trevisan’s extractor consists in a structure made of two algorithms: the *weak design* and the *one-bit extractor*; taking as inputs a *weak randomness source*, in our case the  $2n$  raw bits long string, and a seed, which is poly-logarithmic in the input size. The weak design splits the extractor seed into smaller sets, characterized by an overlap  $r$ , which, for our implementation [35], cannot exceed  $2e$ . The smaller  $r$  is, the longer will the final extracted bit string and the required seed be. Then, the one-bit extractor combines the weak randomness source with each seed set and extracts a random bit, composing the final string of random bits (for a detailed description of the classical randomness extractor see Methods). The complete procedure is summarized in Fig.3.

### RESULTS

Our results are summarized in Table I and in Fig.4. The reported violation values were obtained in different experimental conditions, changing the alignment of the Pockels cell. Since each violation value  $\mathcal{I}$  in Tab. I was evaluated through 16390 raw bits, the statistical parameter  $\gamma$  appearing in Eq. 2 is 0.1619, considering a failure probability  $\delta = 0.01$ . Hence, the min-entropy bounds reported in Tab. I correspond to the values  $\mathcal{I}^* - \gamma$ . Setting an error of  $\epsilon = 10^{-7}$  for the classical extractor, we were able to extract a total of 28273 certified

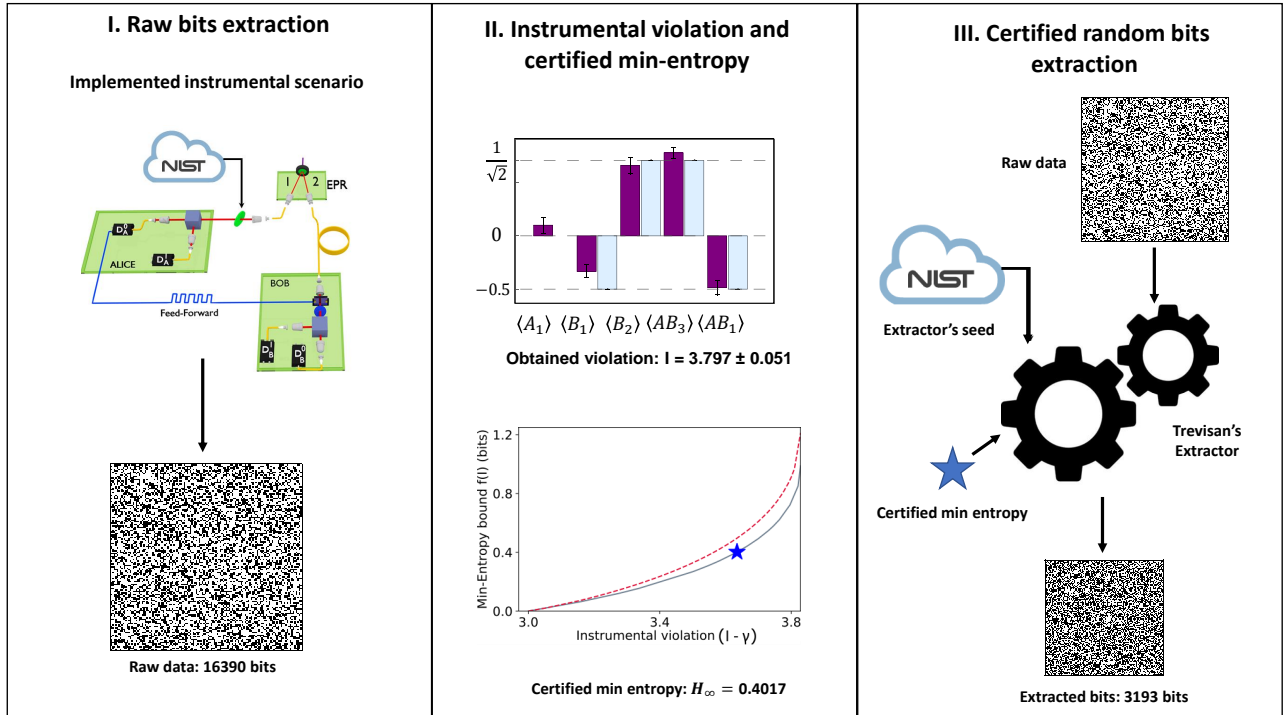


**FIG. 3. Implementation of the Device-Independent randomness certification protocol:** The implementation of our proposed protocol is made up of three steps. First of all, an instrumental process is implemented on a photonic platform and Alice’s and Bob’s outcomes are taken as the bits forming the raw data string (in the image, the string of raw bits is represented through a square made of  $n$  pixels, where black and white encode the two possible values). Secondly, through these collected bits, we evaluate the corresponding instrumental violation and subtract the statistical error  $\gamma$ , that, in our case, amounts to 0.1619. Then, we evaluate the min-entropy corresponding to the obtained value of instrumental violation minus  $\gamma$ , which characterizes our string of raw data. This is done through the curve given by the NPA method (see Methods), corresponding to  $\chi=1$ , which is the worst-case scenario (lowest min-entropy bound), and multiplying it for the number of performed experimental runs. In the third stage, we employ the Trevisan extractor, to extract the final certified random bit string. The extractor takes, as input, the raw data (weak randomness source), a random seed (given by the NIST Randomness Beacon) and the min-entropy of the input string. In the end, according to the min-entropy the error ( $\epsilon$ ) threshold set by the user (in our case  $10^{-7}$ ), the algorithm extracts  $m$  truly random bits, with  $m < n$ .

random bits. The ratio between the extracted bits and the maximum amount of bits that could be in principle extracted after  $n$  runs, given by  $n \times \mathcal{H}_\infty$  is shown in Fig. 4b. The length of the seed, as mentioned, is poly-logarithmic in the input size and it also depends on  $\epsilon$  and on the particular algorithm chosen as *weak design* (see Supplemental Material, Figure 3). In our case, we chose the *block weak design* algorithm [35], which, with respect to other algorithms, requires a longer seed, but allows to extract more random bits. For more details about the internal functioning of the classical randomness extractor and its specific parameter settings, see the Methods section and Supplemental Material.

## DISCUSSION

In conclusion, in this work, we bring a proof-of-principle demonstration that the instrumental process can generate and certificate random bits in device independent fashion, consti-

tuting an alternative venue with respect to Bell-like scenarios. Indeed, the obtained relation between the instrumental violation and min-entropy characterizing the output string requires no assumptions on the quantum state being measured nor on the internal functioning of Alice’s and Bob’s measurement devices. It only requires that the implemented causal structure is an instrumental process, i.e. in particular, that the instrument is affecting Bob’s choice only through Alice’s outcome ( $X$  has no direct causal influence over  $B$ ). We do not require the iid assumption either.

Through our protocol, summarized in Fig. 1-c and 3 and implemented on a photonic platform, we were able to extract an overall number of 28273 certified random bits (summing up the values reported in the fifth column of Table I). The highest conversion rate we were able to reach, from public (input) to private (output) randomness ( $N_{extr}/(N_{trits} \times \log_2(3))$ ) of  $\sim 0.25$ , since 180290 trits were injected to the apparatus. Considering that each experimental round lasted 1s, the maximum extraction rate, given by  $N_{extr}/(N_{run} \times$

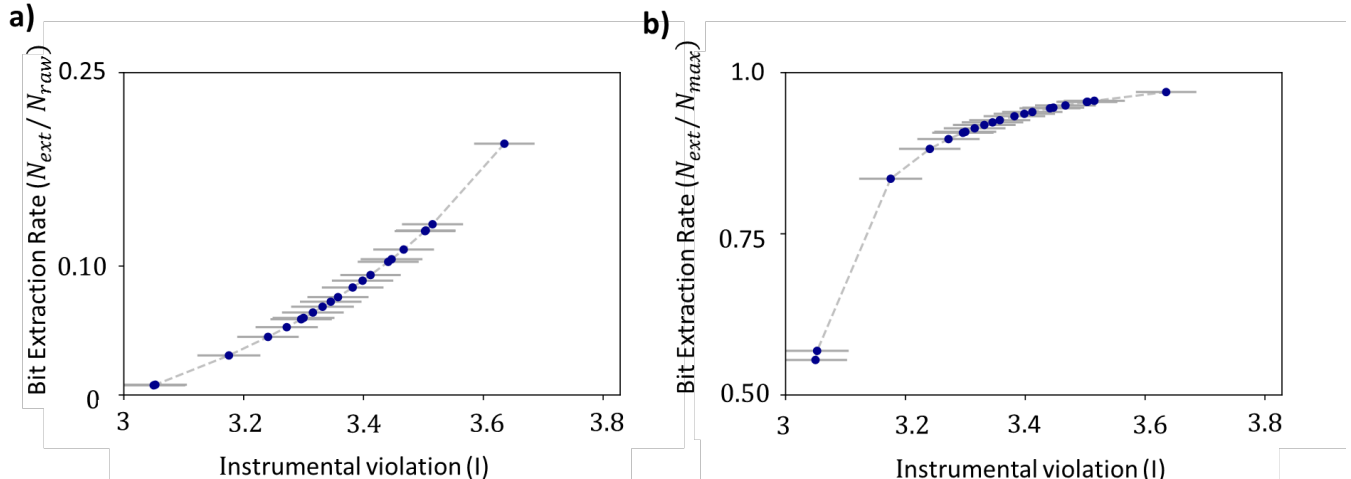


FIG. 4. **Random bits extraction rate:** In these plots we show the ratio of the extracted bits adopting the Trevisan classical randomness extractor. Panel (a) corresponds to the extractor over raw bits collected from the experimental apparatus; whereas panel (b) over the maximum amount of bits that could be extracted according to their certified min-entropy. The exact number of extracted bits for each obtained value of the instrumental violation is included in Tab. I

$\Delta t_{run}$ ), was of 0.328 Hz, we considered an upper bound for  $\Delta t_{run}$  of 1s. Note that the bottleneck of our implementation, which prevents us to reach higher rates, is the time response of the liquid crystal, that implements Alice’s operator and makes  $\Delta t \sim 700ms$ . Hence, these rates could be higher if Alice’s measurement station was implemented with an electro-optical fast device, with shorter response times. We also notice that, as seen in Fig. 1-b, the randomness generated is different for each input  $x$ . This suggests that, in principle, more randomness could be obtained if the best input was chosen more often [38]. Let us note that our experimental implementation requires the *fair sampling* assumption, due to our overall low detection efficiency. Moreover, in the present paper, we adapt the techniques developed by Pironio et al. [4], which is secure against a classical malicious adversary. The same security assumption is made also in [16, 32]. Only very recently the ultimate solution for unconditional security, included finite statistics and non-iid, was given for the Bell scenario [17]. We expect that the same techniques are applicable to the instrumental scenario.

This proof-of-principle opens the path for further investigations of the instrumental scenario as a possible venue for other information processing tasks usually associated to Bell scenarios, such as self-testing [39–48] and communication complexity problems [49–51].

## ACKNOWLEDGEMENTS

We acknowledge support from John Templeton Foundation via the grant Q-CAUSAL n°61084 (the opinions expressed in

this publication are those of the authors and do not necessarily reflect the views of the John Templeton Foundation). IA, DP, MM, GC and FS acknowledge project Lazio Innova SINFO-NIA. DC acknowledges a Ramon y Cajal fellowship, Spanish MINECO (Severo Ochoa SEV-2015-0522), Fundació Privada Cellex and Generalitat de Catalunya (CERCA Program). LG and LA acknowledge financial support from the São Paulo Research Foundation (FAPESP) under grants 2016/01343-7 and 2018/04208-9. RC acknowledges the Brazilian ministries MCTIC, MEC and the CNPq (grants No. 307172/2017 – 1 and 406574/2018 – 9 and INCT-IQ) and the Serrapilheira Institute (grant number Serra-1708-15763). G.C. acknowledges Conicyt and Becas Chile. LA acknowledges financial support also from the Brazilian agencies CNPq (PQ grant No. 311416/2015-2 and INCT-IQ), FAPERJ (JCNE E-26/202.701/2018), CAPES (PROCAD2013 project), and the Brazilian Serrapilheira Institute (grant number Serra-1709-17173).

## METHODS

### Experimental details

Photon pairs were generated in a parametric down conversion source, composed by a nonlinear crystal beta barium borate (BBO) of 2 mm-thick injected by a pulsed pump field with  $\lambda = 392.5$  nm. After spectral filtering and walk-off compensation, photons of  $\lambda = 785$  nm are sent to the two measurement stations A and B. The crystal used to implement active feed-forward is a  $\text{LiNbO}_3$  high-voltage micro Pockels Cell –

Instrumental violation ( $\mathcal{I}^*$ )	Standard Deviation	$\mathcal{H}_\infty$	Extracted Bits	Extractor's seed length	Extraction rate (Hz)
3.1587	0.0528	0	0	0	0
3.2117	0.0528	0.0185	52	32768	0.0065
3.2144	0.0528	0.0196	61	32768	0.0075
3.3372	0.0525	0.0710	483	131072	0.0590
3.4025	0.0513	0.1023	739	163840	0.0902
3.4337	0.0519	0.1184	870	180224	0.1063
3.4578	0.0512	0.1313	977	196608	0.1193
3.4618	0.0517	0.1335	995	196608	0.1215
3.4774	0.0515	0.1423	1066	196608	0.1302
3.4935	0.0523	0.1515	1142	196608	0.1395
3.5072	0.0513	0.1596	1209	212992	0.1475
3.5193	0.051	0.1669	1269	212992	0.1549
3.5438	0.0514	0.1822	1394	212992	0.1702
3.5603	0.0512	0.1930	1482	229376	0.1809
3.5736	0.0504	0.2018	1555	229376	0.1898
3.6031	0.0509	0.2224	1723	229376	0.2103
3.6087	0.0516	0.2265	1756	245760	0.2144
3.6289	0.0507	0.2415	1880	245760	0.2294
3.6646	0.0508	0.2698	2111	245760	0.2577
3.6658	0.0497	0.2708	2119	262144	0.2587
3.6771	0.0510	0.2803	2197	262144	0.2682
3.7970	0.0505	0.4017	3193	294912	0.3897

TABLE I. **Extracted certified random bits.** In this table, we show the obtained results, given by our randomness generator and certifier. Starting from the left, the first and second columns contain all the obtained instrumental violations each of them through 16390 experimental runs, with their standard deviations, estimated through Poissonian error on the coincidence counts propagated. The third column shows the min-entropy in the worst-case (i.e.  $x=1$ ), through the NPA method (see Methods), corresponding to each violation ( $\mathcal{I}^*$ ) minus the statistical parameter  $\gamma$  of Eq.2, which, for a failure probability  $\delta = 0.01$ , amounts to 0.1619. The fourth column shows the number of raw bits, while in the fifth and sixth, there is the number of bits extracted, through the *Block-weak design* algorithm (see Supplementary material) within the classical randomness extractor, setting an error of  $\epsilon = 10^{-7}$ , which required the seed lengths shown in the fifth column. In the sixth column, we are showing the extraction rate, i.e. the number of extracted bits per second, considering that each measurement run lasted at most 1s.

made by Shanghai Institute of Ceramics with  $< 1$  ns risetime and a fast electronic circuit transforming each Si-avalanche photodetection signal into a calibrated fast pulse in the kV range needed to activate the Pockels Cell– is fully described in [52]. To achieve the active feed-forward of information, the photon sent to Bob's station needs to be delayed, thus allowing the measurement on the first qubit to be performed. The amount of delay was evaluated considering the velocity of the signal transmission through a single mode fiber and the activation time of the Pockels cell. We have used a fiber 125 m long, coupled at the end into a single mode fiber that allows a delay of 600 ns of the second photon with respect to the first.

#### NPA method applied to the instrumental scenario

In order to estimate the randomness in the instrumental scenario we adapted the numerical method proposed in [4], which is valid for the Bell scenario. The idea is to consider that additionally to Alice and Bob, there exists a third observer, Eve, that is trying to guess Alice and Bob's outcomes. The three observers share a tripartite state  $|\Psi_{ABE}\rangle$ , onto which

they perform local measurements. The statistics obtained are then evaluated on an instrumental inequality, which allows us to calculate Eve's maximum guessing probability. Eve is assumed to know  $|\Psi_{ABE}\rangle$  and the measurements implemented by Alice and Bob. In this case, the maximum probability that Eve guesses correctly  $(a, b)$  given that  $x = j$  ( $j = 1, 2, 3$ ), and the value  $\mathcal{I} = \beta$  for the left-hand side of (1) was obtained is

$$\begin{aligned} \max_{a,b} & \sum_{a,b} \langle \Psi_{ABE} | \Pi_{a|x=j} \otimes \Pi_{b|y=a} \otimes \Pi_{e=(a,b)} | \Psi_{ABE} \rangle \\ \text{s.t.} & P(a, b|x) = \langle \Psi_{ABE} | \Pi_{a|x} \otimes \Pi_{b|y=a} \otimes \mathbb{I}_E | \Psi_{ABE} \rangle, \\ & \forall a, b, x \quad \mathcal{I}(\{P(a, b|x)\}) = \beta, \end{aligned}$$

where the maximization is taken over all possible tripartite states  $\Psi_{ABE}$  and local measurements  $\{\Pi_{a|x}\}, \{\Pi_{b|y}\}, \{\Pi_e\}$  to Alice, Bob, and Eve, respectively.

This optimization problem is computationally intractable, as it considers quantum systems of arbitrary dimension. A way out is to upper-bound its value by using the Navascu e-Pironio-Ac ın (NPA) hierarchy [34]. In the standard Bell scenario, the NPA hierarchy is used to generate a sequence of

sets  $\mathcal{Q}_1 \supset \mathcal{Q}_2 \supset \dots$  that converges to the set of quantum behaviours. Here, we adapt it to the instrumental scenario, by addressing Bell behaviours  $\{P(a, b|x, y)\}_{a,b,x,y}$  lying on some level  $\mathcal{Q}_k$  of the hierarchy and imposing extra restrictions solely on the events for which Bob's input matches Alice's output, i.e. on the sub-behaviour  $\{P(a, b|x, y = a)\}_{a,b,x}$ . NPA then ensures that our optimization runs over a superset of the set of quantum behaviours actually originated in an instrumental experiment, while leaving the events  $P(a, b|x, y)$  where  $y \neq a$  as free variables that are not considered in the experiment.

More explicitly, we wish to characterize Alice and Bob's instrumental behaviours that can be obtained as marginals of a tripartite behaviour involving Eve. Hence, our upper-bound approximation to the probability  $P_{guess}(x = j)$  that Eve guesses correctly  $(a, b)$ , given that  $x = j$  ( $j = 1, 2, 3$ ) and that the probabilities  $\{P(a, b, e|x)\}_{a,b,e,x}$  display a violation  $\mathcal{I}(\{\sum_e P(a, b, e|x)\}_{a,b,x}) = \beta$ , is given by

$$\begin{aligned} \max_{P(a,b,e|x,y)} \quad & \sum_{a,b} P(e = (a,b)|x = j, y = a) \quad (3) \\ \text{s.t.} \quad & \{P(a, b|x, y, e = e_0)\} \in \mathcal{Q}_k, \forall e_0 \\ & \mathcal{I}(\{\sum_e P(a, b, e|x, y = a)\}) = \beta. \end{aligned}$$

In our implementation, we used  $k = 2$ .

The optimal value  $P_{guess}(x = j)$  of the above SDP is used to define  $f_{x=j}(\mathcal{I}) = -\log_2(P_{guess}(x = j))$  in the lower bound  $H_\infty(A, B|E, x = j) \geq f_{x=j}(\mathcal{I})$  mentioned in the main text.

### Classical Randomness Extractor

Given a string of  $n$  bits, characterized by min-entropy  $k$ , with  $k = \alpha n$ , where  $\alpha$  is the min-entropy per bit, a *quantum-proof*  $(k, \epsilon)$ -*extractor* is a deterministic function which, taking the string as input (the so-called (*weak*) *random source*), along with a uniformly distributed seed made of  $d$  bits, outputs a  $m$ -bit long string  $\epsilon$ -close to uniform. The strength of a randomness extractor depends on two quantities: (i) the so-called *entropy loss*, given by  $k - m$ , and (ii) the bit-length  $d$  of the seed. Both these parameters should be optimized, since the goal is to minimize the losses while consuming the smallest possible amount of randomness.

Recently, a promising randomness extractor, Trevisan's extractor [27], has attracted considerable theoretical interest since it has been proven to be secure against quantum adversaries [53]. The seed length of Trevisan's extractor is poly-logarithmic in the size of the input, greatly outperforming randomness extractors based on (almost) universal hashing, which are the most often used in quantum cryptography but require a seed whose size scales linearly with the length of the input. Trevisan's extractor has been also proven to be a strong extractor [54], i.e., the seed is almost independent of the final

output, so the randomness of the seed is not consumed by the process and can be reused as part of the result.

Implementations of this extractor were made by Ma *et al.* [55], Maurer *et al.* [35], and more recently by Shen *et al.* [18]. The extraction protocol is composed by two parts: (i) the *weak design*, that divides the initial seed into smaller blocks of random bits of length  $t$  and (ii) the *one bit extractor*, which extracts a single random bit from the random source for each block.

In the *weak design*, the blocks  $\{S_1, \dots, S_j\}$  into which the seed is divided should be nearly independent to ensure that the maximum amount of entropy is extracted. Hence, a family of sets  $S_1, \dots, S_m \subset [d]$  is a *weak*  $(m, t, r, d)$ -*design* if

1. For all  $i$ ,  $|S_i| = t$
2. For all  $i$ ,  $\sum_{j=1}^{i-1} 2^{|S_j \cap S_i|} \leq rm$ , where the parameter  $r$  is the so-called *overlap* of the weak design.

Each of the  $S_j$  is fed into a one bit extractor and they are all finally concatenated into a string to form the extracted randomness.

In our work, we adopted two types of weak design. The first, which we will refer to as the *standard weak design*, is a refined version of Nisan and Wigderson [56], whose effectiveness was proved by Hartman and Raz [57], under the parameters choice given by  $r = 2e$  and  $d = t^2$  with  $t = 2\lceil \log n + 2 \log 2/\epsilon \rceil$ . The second, called *block weak design*, is a design from Ma and Ta [58] modified by Maurer *et al.* [35] with  $r = 1$  and  $d = (l + 1)t^2$ , where  $l := \max\{1, \lceil \frac{\log(m-r') - \log(t-r')}{\log(r') - \log(r'-1)} \rceil\}$  and  $r' = 2e$ . In comparison, the second design requires a seed's length exceeding the input weak random source's string's length, but it allows to extract more bits from the source, due to a smaller  $r$ . The one-bit extractor is realized by an error correcting code, which is constructed by concatenating a Reed-Solomon code with an Hadamard code. Hence, as a preliminary step, we fix the following three parameters: (i)  $n$  (input length), (ii)  $\alpha$  (min-entropy per bit, certified by the experimental instrumental violation, see Fig.1-c and Fig.3) and (iii)  $\epsilon$  (error per bit). After that, we derive the seed length, the total min-entropy  $k = \alpha n$ , and  $m = (k - 4 \log \frac{1}{\epsilon} - 6)/r$  (according to the one-bit extractor). Intuitively, the smaller the cardinality of the intersections of the sets  $\{S_i\}$ , the smaller will be the required min-entropy required to obtain the same length  $m$  of the output string.

- 
- [1] Grangier P. and Auffèves A. *What is quantum in quantum randomness?* *Phil. Trans. R. Soc. A* **376** 20170322 (2018)
  - [2] Matsumoto M. and Nishimura T. *623-dimensionally equidistributed uniform pseudo-random number generator.* *ACM Trans. Model. Comput. Simul.* **8**, 3-30, (1998).
  - [3] Rukhin A. *A statistical test suite for random and pseudo-random numbers generators for cryptographic applications* *arXiv:quant-ph/0606049v4* (2009)
  - [4] Pironio S., Acín A., Massar S., De La Giroday A. B., Matsukevich D. N., Maunz P., Olmschenk S., Hayes D., Luo L. and

- Manning T.A. *Random numbers certified by Bell's theorem Nature* 464, 10, (2010).
- [5] Clauser J.F., Horne M.A., Shimony A., Holt R.A. *Proposed experiment to test local hidden-variable theories Phys. Rev. Lett.* 23, 15: 880-884, (1969).
- [6] R. Ramanathan, F. G. S. L. Brandão, K. Horodecki, M. Horodecki, P. Horodecki, and H. Wojewódka *Randomness Amplification under Minimal Fundamental Assumptions on the Devices Physical Review Letters* 117, 230501, (2016).
- [7] R. Colbeck, and R. Renner *Free Randomness Can Be Amplified Nature Physics* 8, 450-453, (2012).
- [8] R. Gallego, L. Masanes, G. De La Torre, C. Dhara, L. Aolita, and Antonio Acín *Full randomness from arbitrarily deterministic events Nature Communications* 4, 2654, (2013).
- [9] F. G. S. L. Brandão, R. Ramanathan, A. Grudka, K. Horodecki, M. Horodecki, P. Horodecki, T. Szarek, and H. Wojewódka *Realistic noise-tolerant randomness amplification using finite number of devices Nature Communications* 7, 11345, (2012).
- [10] Miller C. A., and Shi Y. *Robust protocols for securely expanding randomness and distributing keys using untrusted quantum devices Journal of the ACM* 63, Issue 4, 33, (2016).
- [11] Vazirani U., and Vidick T. *Certifiable Quantum Dice - Or, testable exponential randomness expansion Proc. of the 44th annual ACM Symposium on Theory of computing* 61-66, (2012).
- [12] Y. Liu, X. Yuan, M.-H Li, W. Zhang, Q. Zhao, J. Zhong, Y. Cao, Y.-H. Li, L.-K. Chen, H. Li, T. Peng, Y.-A. Chen, C.-Z. Peng, S.-C. Shi, Z. Wang, L. You, X. Ma, J. Fan, Q. Zhang, and J.-W. Pan *High-Speed Device-Independent Quantum Random Number Generation without a Detection Loophole Phys. Rev. Lett.* 120, 010503, (2018).
- [13] U. Vazirani, T. Vidick *Fully Device-Independent Quantum Key Distribution Phys. Rev. Lett.* 113, 140501, (2016).
- [14] K.-M. Chung, Y. Shi, X. Wu *Physical Randomness Extractors: Generating Random Numbers with Minimal Assumptions arXiv:1402.4797* (2015).
- [15] F. Dupuis, O. Fawzi, and R. Renner *Physical Randomness Extractors: Generating Random Numbers with Minimal Assumptions arXiv:1402.4797* (2016).
- [16] B. G. Christensen, K. T. McCusker, J. B. Altepeter, B. Calkins, T. Gerrits, A. E. Lita, A. Miller, L. K. Shalm, Y. Zhang, S. W. Nam, N. Brunner, C. C. W. Lim, N. Gisin, and P. G. Kwiat *Detection-Loophole-Free Test of Quantum Nonlocality, and Applications Phys. Rev. Lett.* ] (2013).
- [17] R. Arnon-Friedman, R. Renner, T. Vidick *Simple and tight device-independent security proofs SIAM Journal on Computing* 48.1: 181-225 (2019).
- [18] L. Shen, J. Lee, L. P. Thinh, and J.-D. Bancal, A. Cerè, A. Lamas-Linares, A. Lita, T. Gerrits, S. W. Nam, V. Scarani, and C. Kurtsiefer *Randomness extraction from Bell violation with continuous parametric down-conversion. Phys. Rev. Lett.* 121, 150402, (2018).
- [19] P. Bierhorst, E. Knill, S. Glancy, Y. Zhang, A. Mink, S. Jordan, A. Rommal, Y.-K. Liu, B. Christensen, S. W. Nam, M. J. Stevens, and L. K. Shalm *Experimentally generated randomness certified by the impossibility of superluminal signals Nature* 556, 223-226, (2018).
- [20] R. Chaves, R. Kueng, J.B. Brask, and D. Gross *Unifying Framework for Relaxations of the Causal Assumptions in Bell's Theorem Phys. Rev. Lett.* 114, 140403, (2015).
- [21] Wood, Christopher J., and Robert W. Spekkens *The lesson of causal discovery algorithms for quantum correlations: Causal explanations of Bell-inequality violations require fine-tuning New Journal of Physics* 17, 033002, (2015).
- [22] Judea Pearl *Causality Cambridge University Press, Cambridge* (2009).
- [23] Gonzalo Carvacho, Rafael Chaves, and Fabio Sciarrino. *Perspectives on experimental quantum causality. Europhysics Letters* 125, 36, (2019).
- [24] Rafael Chaves, Gonzalo Carvacho, Iris Agresti, Valerio Di Giulio, Leandro Aolita, Sandro Giacomini and Fabio Sciarrino. *Quantum violation of an instrumental test. Nature Physics* 14 291-296, (2018).
- [25] Judea Pearl *On the Testability of Causal Models with Latent and Instrumental Variables Proceedings of the 11th conference on Uncertainty in artificial intelligence (UAI '95)* 435-443 (1995).
- [26] Blai Bonet *Instrumentality Tests Revisited Proceedings 17th Conference Uncertainty in Artificial Intelligence* 48-55 (2001).
- [27] L. Trevisan, *Extractors and pseudorandom generators J. ACM* 48, 860-879, (2001).
- [28] Bell J.S. *On the Einstein Podolsky Rosen Paradox Physics* 1 (3) (1964).
- [29] T. Van Himbeek, J. Bohr Brask, S. Pironio, R. Ramanathan, A. B. Sainz, E. Wolfe *Quantum violations in the Instrumental scenario and their relations to the Bell scenario arXiv:1804.04119* (2018).
- [30] Stefano Pironio and Serge Massar *Security of practical private randomness generation. Phys. Rev. A* 87, 012336, (2013).
- [31] O. Nieto-Silleras, S. Pironio, and J. Silman *Using complete measurement statistics for optimal device-independent randomness evaluation. New J. Phys.* 16, 013035, (2014).
- [32] Jean-Daniel Bancal, Lana Sheridan, and Valerio Scarani *More randomness from the same data. New J. Phys.* 033011, (2014).
- [33] Aaronson S., and Gross R. *Bounding the seed length of Miller and Shi's unbounded randomness expansion protocol. arXiv:1410.8019* 48-55 (2014).
- [34] Miguel Navascués, Stefano Pironio and Antonio Acín *Bounding the Set of Quantum Correlations. Phys. Rev. Lett.* 98, 010401, (2007).
- [35] W. Mauerer, C. Portmann, and V. B. Scholz, *A modular framework for randomness extraction based on Trevisan's construction arXiv:1212.0520v1* (2012).
- [36] Our implementation of Trevisan extractor can be found at the following link: <https://github.com/michelemancusi/libtrevisan> (2019).
- [37] M. J. Fischer, M. Iorga, R. Peralta *A public randomness service. Proc. International Conf. on Security and Cryptography* 434-438, (2011).
- [38] Nieto-Silleras, O. and Bamps, C. and Silman, J. and Pironio, S. *Device-independent randomness generation from several Bell estimators. New Journal of Physics* 2, 023049, (2018).
- [39] D. Mayers, and A. Yao *Self-testing quantum apparatus Quantum Information & Computation* 4, 273, (2004).
- [40] T. H. Yang, and M. Navascués *Robust self-testing of unknown quantum systems into any entangled two-qubit states Physical Review A* 87, 050102, (2013).
- [41] M. McKague, T. H. Yang, and V. Scarani *Robust self-testing of the singlet J. Phys. A: Math. Theor.* 45, 455304, (2014).
- [42] C. Bamps, and S. Pironio *Sum-of-squares decompositions for a family of Clauser-Horne-Shimony-Holt-like inequalities and their application to self-testing Phys. Rev. A* 91, 052111, (2015).
- [43] X. Wu, J. D. Bancal, M. McKague, and V. Scarani *Device-independent parallel self-testing of two singlets Phys. Rev. A* 93, 062121, (2016).
- [44] I Šupić, R Augustiak, A Salavrakos, A Acín *Self-testing protocols based on the chained Bell inequalities. New Journal of Physics* 18(3), 035013, (2016).

- [45] A. Coladangelo, K. T. Goh, and V. Scarani *All pure bipartite entangled states can be self-tested* *Nat. Commun.* **8**, **15485**, (2017).
- [46] M. McKague *Self-testing in parallel with CHSH* *Quantum* **1**, **1**, (2017).
- [47] I. Šupic, A. Coladangelo, R. Augusiak, and A. Acín *Self-testing multipartite entangled states through projections onto two systems* *New Journal of Physics* **20**, **083041**, (2018).
- [48] J. Bowles, I. Šupic, D. Cavalcanti, and A. Acín *Device-independent randomness generation from several Bell estimators* *Physical Review A* **98**, **042336**, (2018).
- [49] C. Brukner, M. Zukowski, J.-W. Pan, A. Zeilinger *Bell's inequalities and quantum communication complexity* *Physical Review Letters* **92**(12):**127901**., (2004).
- [50] H. Buhrman, R. Cleve, S. Massar, R. de Wolf *Nonlocality and communication complexity* *Rev. Mod. Phys.* **82**(1):**665**, (2010).
- [51] H. Buhrman, Ł. Czekaj, A. Grudka, M. Horodecki, P. Horodecki, M. Markiewicz, Fl. Speelman, and S. Strelchuk *Quantum communication complexity advantage implies violation of a Bell inequality* *PNAS* **113** (12), **3191-3196**, (2016).
- [52] S. Giacomini, F. Sciarrino, E. Lombardi, and F. De Martini *Active Teleportation of a quantum bit* *Phys. Rev. A* **66**, **030302**, (2002).
- [53] A. De, C. Portmann, T. Vidick, and R. Renner, *Trevisan's extractor in the presence of quantum side information* *SIAM J. Comput.* **441**, **915-940**, (2012).
- [54] R. Raz, O. Reingold, and S. Vadhan, *Extracting all the randomness and reducing the error in Trevisan's extractors* *Proc 31st ACM Symp Theory of Computing* **149-158**, (1999).
- [55] X. Ma, F. Xu, H. Xu, X. Tan, B. Qi, and H.-K. Lo, *Postprocessing for Quantum Random-Number Generators: Entropy Evaluation and Randomness Extraction* *Phys. Rev. A* **87**, **062327**, (2013).
- [56] N. Nisan, and A. Wigderson, *Hardness vs randomness* *Journal of Computer and System Sciences* **49**, **149-167**, (1994).
- [57] T. Hartman, and R. Raz, *On the distribution of the number of roots of polynomials and explicit weak design* *Random Structures and Algorithms* **23**, **235-263**, (2003).
- [58] Xiongfeng Ma and Xiaoqing Tan, *Explicit combinatorial design* [arXiv:1109.6147](https://arxiv.org/abs/1109.6147), (2012).

## Supplementary Information

### Experimental device-independent certified randomness generation with an instrumental causal structure

Iris Agresti,<sup>1</sup> Davide Poderini,<sup>1</sup> Leonardo Guerini,<sup>2</sup> Michele Mancusi,<sup>1</sup> Gonzalo Carvacho,<sup>1</sup> Leandro Aolita,<sup>2,3</sup> Daniel Cavalcanti,<sup>4</sup> Rafael Chaves,<sup>5,6</sup> and Fabio Sciarrino<sup>1</sup>

<sup>1</sup>*Dipartimento di Fisica, Sapienza Università di Roma, Piazzale Aldo Moro 5, I-00185 Roma, Italy*

<sup>2</sup>*International Center of Theoretical Physics - South American Institute for Fundamental Research, Instituto de Física Teórica - UNESP, R. Dr. Bento T. Ferraz 271, 01140-070, São Paulo, Brazil*

<sup>3</sup>*Instituto de Física, Universidade Federal do Rio de Janeiro, Caixa Postal 68528, Rio de Janeiro, RJ 21941-972, Brazil*

<sup>4</sup>*ICFO - Institut de Ciències Fotoniques, The Barcelona Institute of Science and Technology, E-08860 Castelldefels, Barcelona, Spain*

<sup>5</sup>*International Institute of Physics, Federal University of Rio Grande do Norte, 59078-970, P. O. Box 1613, Natal, Brazil*

<sup>6</sup>*School of Science and Technology, Federal University of Rio Grande do Norte, 59078-970 Natal, Brazil*

#### Randomness Extractor

Quantum correlations can be exploited to generate random numbers, whose randomness can be device-independently certified. However, in real experimental conditions, quantum correlations are inevitably mixed with classical noise, which could be controlled and used by an adversary (Eve) to gain partial information about the output random bits. This is the reason why there is the need to apply a post-processing procedure to filter the true randomness out of the raw bits generated by a Quantum Random Numbers Generator (QRNG). This procedure is called *randomness extraction* and it involves the use of classical algorithms known as *randomness extractors* [1, 2]. The aim of these algorithms is to obtain a bit sequence, following an "almost uniform" distribution, up to an error parameter  $\epsilon$ , which can be made arbitrarily small. The inputs of a randomness extractors are the following: a weak randomness source, constituted by the raw bits and characterized by a min-entropy of at least  $k$  and a seed of length  $d$ , not necessarily uniform [3]. The accuracy of the extractor can be increased, for a given min-entropy  $k$ , by reducing the number of extracted bits and by injecting a longer seed.

The *min-entropy* of a string  $X$  is a randomness quantifier and it is defined by  $H_{\min}(X) = -\log(\max_x p(X = x))$ , where  $\max_x p(X = x)$  is the *guessing probability*. However, this definition does not consider the possible presence of side information ( $E$ ) correlated to the source  $X$ , as it may happen in more complex settings. The notions of guessing probability and min-entropy consequently need to be extended such that they measure the randomness of the source *conditioned on  $E$* , which, in a cryptographic context, represents the adversary's information about the source.

Hence, mathematically, the task can be expressed by requiring that the joint state of the output and the side information  $\rho_{ZE}$  is  $\epsilon$ -close to  $\tau \otimes \rho_E$  (where  $\tau$  is the fully mixed state and  $\rho_E$  the side information). Specifically, by definition, two probability distributions  $X$  and  $Y$  over the same set  $T$  are  $\epsilon$ -close if the statistical distance between them is bounded by  $\epsilon$ :

$$\|X - Y\| := \frac{1}{2} \sum_{v \in T} |P(X = v) - P(Y = v)| \leq \epsilon. \quad (S1)$$

Assuming that the inputs are bit strings of length  $n$  with min-entropy of at least  $k$ , processed by  $d$  randomly distributed bits (seed), the output is made by  $m$  bit-long strings, according to a probability distribution  $\epsilon$ -close to uniform and independent from the side information. A deterministic function which takes as inputs the source and the seed and achieve these goals is called *quantum-proof  $(k, \epsilon)$ -extractor*. The optimum situation, therefore, would be to have  $m$  as close to  $k$  as possible, meaning that all the available min-entropy has been extracted (indeed  $k - m$  is the *entropy loss*), and the seed, of length  $d$ , as small as possible, to minimize the amount of additional randomness.

Recently, an important and promising randomness extractor, Trevisan's extractor [4], has aroused considerable theoretical interest, since it has been proven to be secure against quantum adversaries [5]. The seed length of Trevisan's extractor is polylogarithmic in the length of the input, greatly outperforming randomness extractors based on (almost) universal hashing, which are now more widely used in quantum cryptography, although they require a seed-size scaling polynomially in the length of the raw input. Furthermore, Trevisan extractor is also proven to be a strong extractor [6], i.e. the seed is almost independent of the final output and so that the randomness in the seed is not consumed in the process (compared to weak extractors) and can be reused as part of the result. Two implementations of this extractor were made by Ma *et al.* [7] and Maurer *et al.* [8].

Trevisan's construction, in a few words, is a recipe to build a randomness extractor combining two elements: a *one bit extractor* and a *weak design* algorithms, as it is shown by the pseudo-code in paragraph *Implementation Details*. The weak design expands the initial seed and divides it into different smaller packets with a certain overlap. Hence, the cumulative length of

the packets can considerably exceed the seed length. By definition, a family of sets  $S_1, \dots, S_m \subset [d]$  is a *weak*  $(m, t, r, d)$ -*design* if

1. For all  $i$ ,  $|S_i| = t$
2. For all  $i$ ,  $\sum_{j=1}^{i-1} 2^{|S_j \cap S_i|} \leq rm$

where the parameter  $r$  is the so-called *overlap* of the weak design. Then, each packet is fed into a one-bit extractor, which extracts a single random bit from the random source. These bits are finally concatenated into a string to form the extracted random bits. In our case, the one-bit extractor was implemented by an error correcting code, which is constructed concatenating a Reed-Solomon code with an Hadamard code; while the adopted weak design is a refined version of the original construction from Nisan and Wigderson [10].

The extraction algorithm consists in applying multiple times the same one-bit extractor to the input string, using different weakly correlated seeds for each run. The seeds are chosen as sub-strings of some longer seed  $y \in \{0, 1\}^d$ .

Formally, let  $\{S_i\}$  be a family of sets such that for all  $i$ ,  $|S_i| = t$ ,  $S_i \subset [d] = \{1, \dots, d\}$  and  $y_{S_i}$ , the string formed by the bits of  $y$  at the positions given by the elements  $j \in S_i$ , is a string of length  $t$ . For a given one-bit extractor,  $C : \{0, 1\}^n \times \{0, 1\}^t \rightarrow \{0, 1\}$  and such a family  $\{S_i\}$  with  $1 \leq i \leq m$ , Trevisan extractor is defined as the concatenation of the output bits of  $C$ , when used with the seed  $y_{S_i}$ , namely:

$$\text{Ext}(x, y) := C(x, y_{S_1}) \cdots C(x, y_{S_m}). \quad (\text{S2})$$

The performance of the extractor depends on the performance of the one-bit extractor, as well as on the independence of the seeds used for each run of the one-bit extractor. The smaller the cardinality of the intersections of the sets  $\{S_i\}$ , the more randomness can be extract form the source, but the larger the seed required. Furthermore if  $\epsilon$  is the error of the one bit extractor, it is also the error per bit for Trevisan's construction.

### Weak design

As mentioned, the weak design construction we use is a refined version of the one adopted by Nisan and Wigderson [10]. Indeed, Maurer *et al.* [8] proved that this construction is a weak  $(m, t, r, d)$ -design for any prime power  $t$  and any  $m$  and that the best parameter choice, for the overlap  $r$  and seed length  $d$ , is  $r = 2e$  and  $d = t^2$  [8]. Obviously a larger overlap produces a larger entropy loss, so we adopt an iterative construction of the basic design from [11], then adapted by [8], to construct a new design with  $r = 1$ , which is the one we use in this work (known as *block weak design*). The construction of a weak design adopts of polynomials over a finite field  $\text{GF}(t)$ . Every set  $S_p$  is indexed by one such polynomial  $p: \text{GF}(t) \rightarrow \text{GF}(t)$ . To construct a weak  $(m, t, r, d)$ -design we need  $m$  sets, and therefore  $m$  such polynomials, which we take in increasing order of their coefficients. In general, the  $n$ -th polynomial is given by  $p(x) = \sum_{i=0}^c \alpha_i x^i$  with  $\alpha_i = \lfloor (n-1) \rfloor / t^i \bmod t$  and  $c = \lceil \frac{\log m}{\log t} - 1 \rceil$ . The elements of the set  $S_p$  are all the pairs of values  $S_p := \{(x, p(x)) : x \in \text{GF}(t)\}$ . Each set has so  $|S_p| = t$  elements, if we fix  $d = t^2$  then, considering the pair  $(x, p(x))$  as a two-digit number  $(x$  and  $p(x))$  and converting it to base  $t$ , we obtain that the set  $S_p$  contain only elements which are numbers less then  $d$ .

A weak design with  $r = 1$  can be made using repeatedly the previous weak design construction with different values  $m_j$  (but the same  $t$ ), achieving different designs  $W_{B,0}, \dots, W_{B,l}$ . So we can build a new design  $W$  by putting these designs in its diagonal, that is:

$$W = \begin{pmatrix} W_{B,0} & & \\ & \ddots & \\ & & W_{B,l} \end{pmatrix}$$

where  $l$  is defined as

$$l := \max \left\{ 1, \left\lceil \frac{\log(m - r') - \log(t - r')}{\log(r') - \log(r' - 1)} \right\rceil \right\} \quad (\text{S3})$$

letting  $r' = 2e$  be the parameter from the basic construction and  $m$  and  $t$  be fixed to the values required by the one bit extractor. Each design  $W_{B,i}$  is constructed with  $m_i$  sets defined as follows:

$$n_i := \left(1 - \frac{1}{r^l}\right)^i \left(\frac{m}{r^l} - 1\right) \quad 0 \leq i \leq l-1, \quad (\text{S4})$$

$$m_i := \left[ \sum_{j=0}^i n_j \right] - \sum_{j=0}^{i-1} m_j \quad 0 \leq i \leq l-1, \quad (\text{S5})$$

$$m_l := m - \sum_{j=0}^{l-1} m_j. \quad (\text{S6})$$

So the weak design  $W$  has  $d = (l+1)t^2$ . Maurer *et al.* [8] proved that this construction has  $r = 1$ . In the paragraph *Implementation Details* we show the pseudo-code of our version of the weak-design (the full source code is available at <https://github.com/michelemancusi/libtrevisan>).

### One-bit extractor

For the implementation of a one-bit extractor, we exploit the result of [12], which proves that the universal<sub>2</sub> hash functions are good extractors. Indeed, we concatenate two hash functions and use a seed-length of  $2l := t$ . The first is known as polynomial hashing, or alternatively as a Reed-Solomon code. We partition the input string  $x \in \{0, 1\}^n$  in blocks  $x = (x_1, \dots, x_s)$ , each of length  $l$  (if necessary we pad the last string  $x_s$  with 0s). We see each block is an element of a field  $x_i \in \text{GF}(2^l)$ , and evaluate the following polynomial:

$$p_\alpha(x) = \sum_{i=1}^s x_i \alpha^{s-1} \quad (\text{S7})$$

where  $\alpha \in \text{GF}(2^l)$  is the first half of the seed. Then, we combine it with another hash function, sometimes referred to as a *Hadamard code*. This hash function computes the parity of the bitwise product of  $p_\alpha(x)$  and the second half of the seed,  $\beta \in \{0, 1\}^l$ . The output is so  $z = \bigoplus_{i=1}^l \beta_i p_\alpha(x)_i$ . The seed of this one bit extractor has length  $t = 2l = 2\lceil \log n + 2 \log 2/\epsilon \rceil$ , the seed of the complete construction has length  $d = t^2$  and the randomness required is  $k = rm + 4 \log \frac{1}{\epsilon} + 6$ . Hence, the number of extracted bits is given by  $m = \lfloor (k - 4 \log_2(1/\epsilon) - 6)/r \rfloor$ . In Fig.1-8, we show the behaviour of our extractor's parameters.

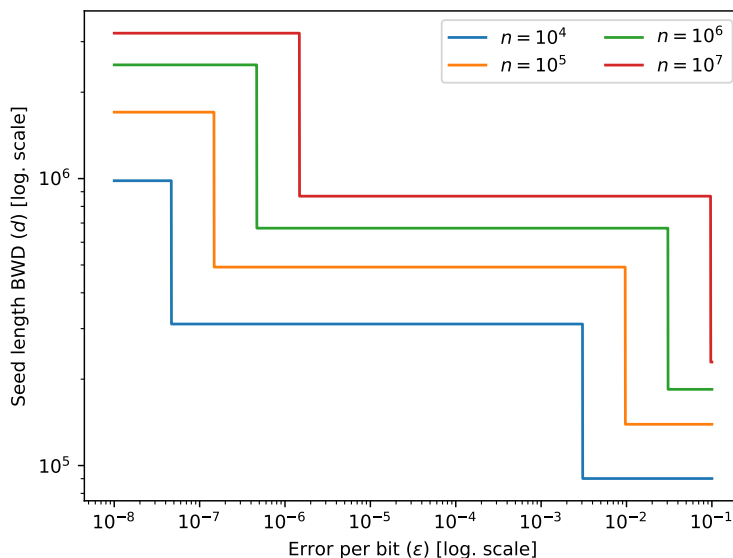


FIG. 1: **Length of the single set  $S$  of the weak design depending on the error per bit.** It can be noted that in semi-log scale, the sub-seed length  $t$  is a step function and decreases linearly as the error per bit  $\epsilon$  increases. Furthermore, the greater the input  $n$ , the greater the length of the single sub-seed created by the weak design.

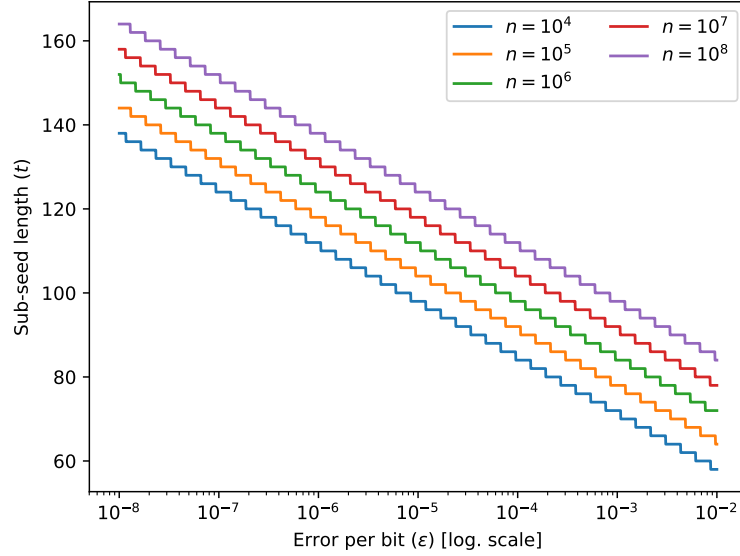


FIG. 2: **Length of the single set  $S$  of the weak design vs the input length of the source.** In this figure is represented how the sub-seed length  $t$  varies as a function of the input length  $n$ , plotted for different error per bit  $\epsilon$  parameters. We can see that in semi-log scale the sub-seed length is a step function and increases linearly with the input. Furthermore, the greater the error per bit, the smaller the length of the single sub-seed created by the weak design.

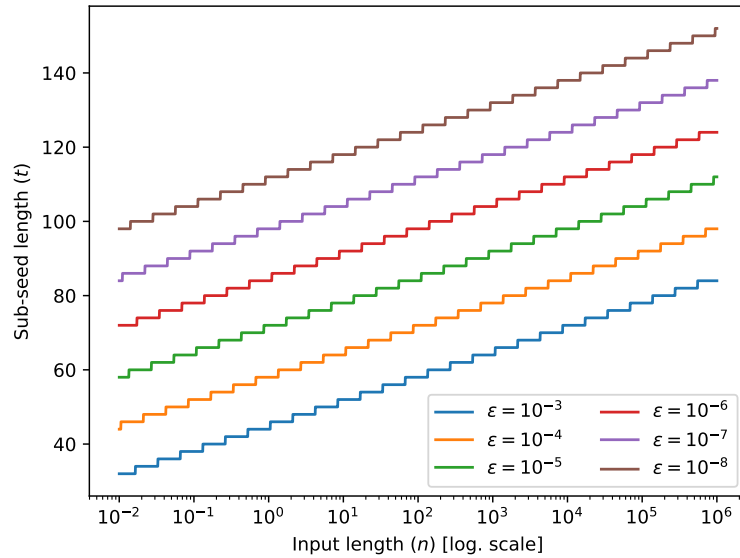


FIG. 3: **Ratio between the output length of the extractor and the error per bit parameter.** This figure shows linear dependence in semi-log scale of the output length  $m$  (multiplied by a constant factor  $r$ ) as a function of the error per bit  $\epsilon$ . Output length increases with the error and the greater the min-entropy  $k$ , the greater the output length.

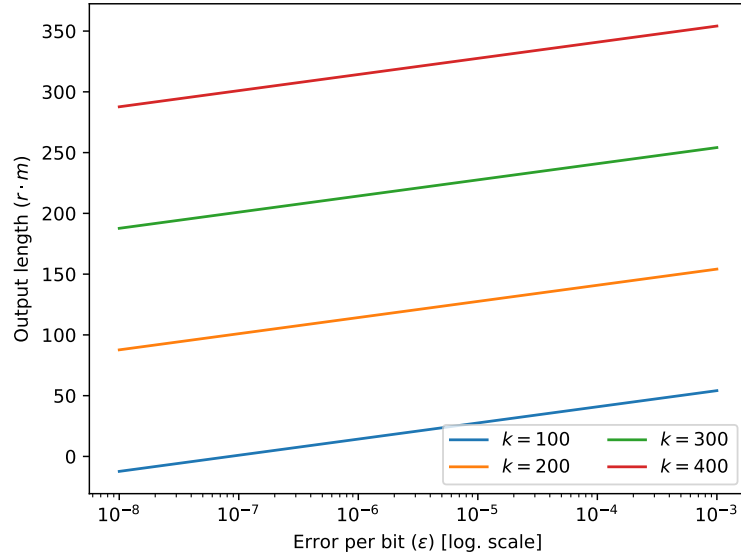


FIG. 4: **Output length vs the min-entropy of the source.** It can be noted that the output length  $m$  (multiplied by a constant factor  $r$ ) is a linear growing monotone function of the min-entropy of the source  $k$  and it also increases with the error per bit  $\epsilon$ .

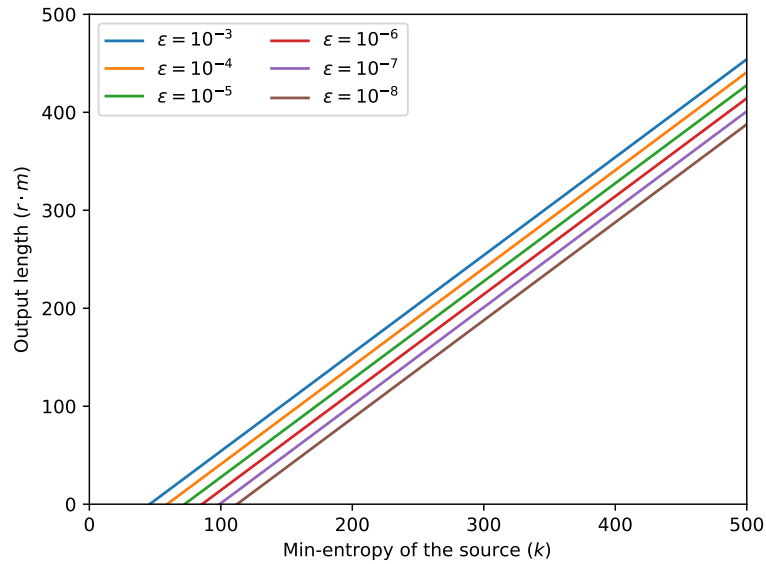


FIG. 5: **Dependency of seed length from the error per bit.** Here different graphs of the seed length  $d$  as a function of the error per bit  $\epsilon$  are plotted, for different input source length in semi-log scale. These functions are step functions and, with the same error, the seed increases with the size of the input  $n$ .

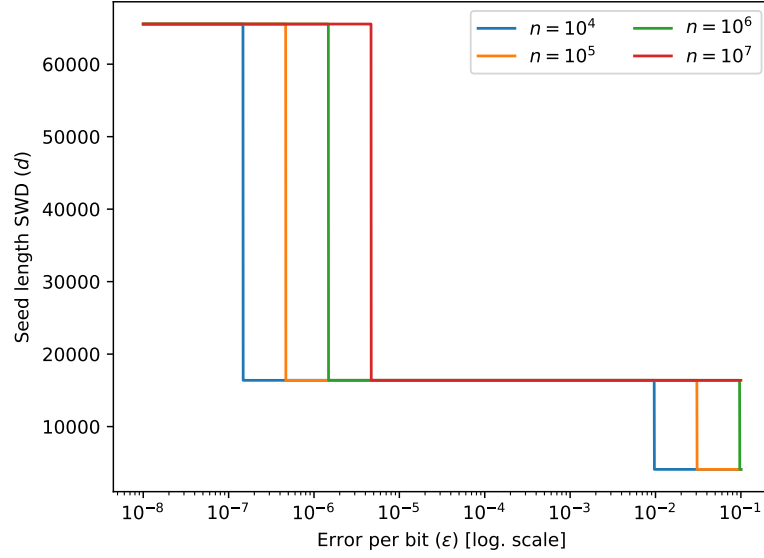


FIG. 6: **Comparison between seed length and the input length of the source.** In this figure is represented the seed length  $d$  vs the input length  $n$  in semi-log scale, plotted for different error per bit  $\epsilon$  parameters. The seed is a step function of the input length, it increases with  $n$  and, with the same input length, the seed length is greater for lower errors.

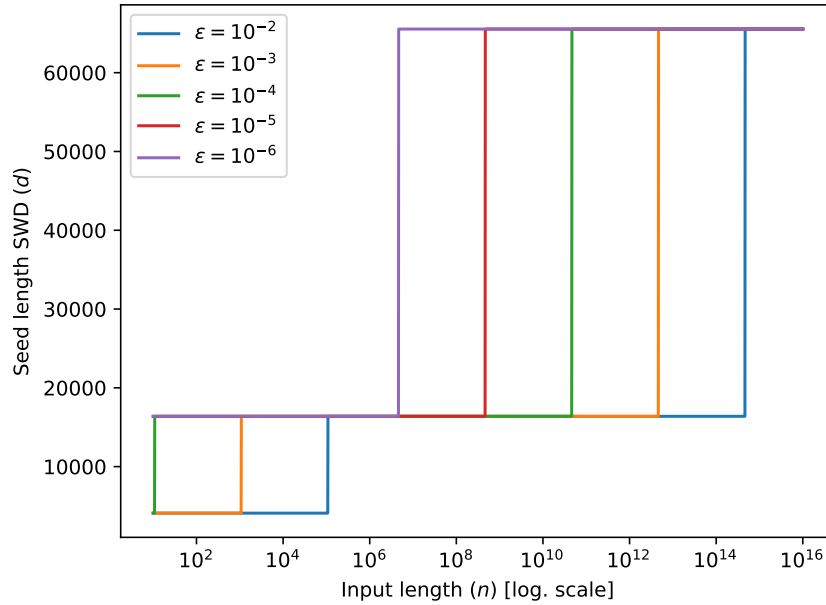


FIG. 7: **Relation between the seed length of block weak design and the input length of the source.** The seed length  $d$  as a function of the input length  $n$  is plotted for different values of min-entropy per bit  $\alpha$  and the error per bit  $\epsilon$  parameter is fixed at  $\epsilon = 10^{-7}$ .  $d$  is a monotone increasing function of  $n$  and it increases also with  $\alpha$ . Both the axes are in logarithmic scale.

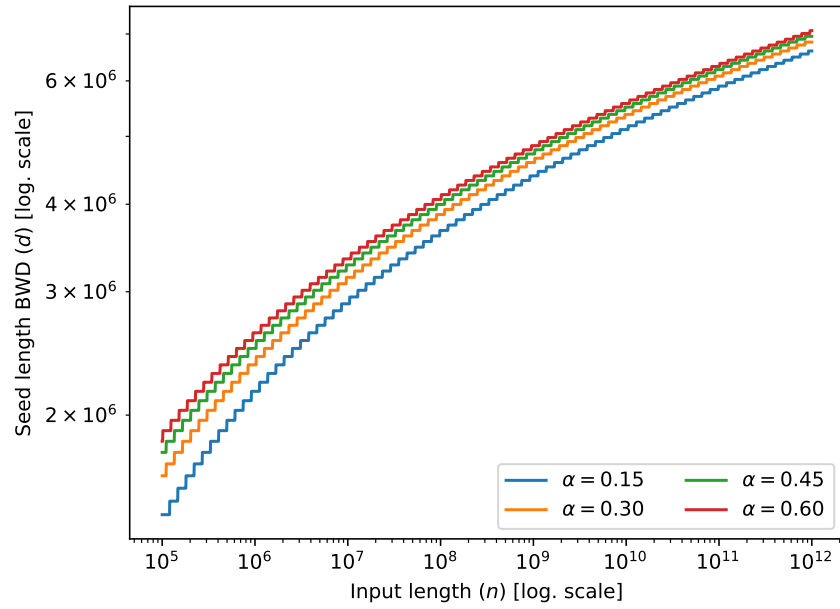


FIG. 8: **Seed length of block weak design depending on the error per bit.** For different input length of the source, the seed length  $d$  as function of the error per bit  $\epsilon$  is plotted.  $d$  is a descending step function of  $\epsilon$ , but it increases with  $n$ . The min-entropy is fixed at  $\alpha = 0.4$  and both the axes are in logarithmic scale.

## Implementation Details

### *Trevisan extractor*

The Trevisan algorithm is independent of the type of weak design and bit extractor used; only the deduced parameters depend on the specific properties of the components.

---

```

1: procedure TREVISAN(WeakDesign, 1-Bit extractor, seed, source,  $n$ ,  $\alpha$ ,  $\epsilon$ )
2:    $k = \alpha \cdot n$ 
3:    $m = \lfloor (k - 4 \log_2(1/\epsilon) - 6)/r \rfloor$  ▷ where  $r = 2e$  or  $r = 1$  depending on the weak design
you use.
4:    $t_{req} = 2 \lceil \log_2(n) + 2 \log_2(2/\epsilon) \rceil$ 
5:    $t = 2^{\lceil \log_2(t_{req}) \rceil}$ 
6:   for  $i < m$  do ▷ where here you can use standard weak design or block
7:      $S = \text{WDcompute}S_i(i, m, t, t_{req})$  weak design
8:      $b = 0$ 
9:     for  $j < t_{req}$  do
10:       $b[j] = \text{seed}[S[i][j]]$ 
11:    end for
12:     $\rho[i] = \text{1-Bit extractor}(b, \text{source}, n, \epsilon)$ 
13:  end for
14:  return  $\rho$ 
15: end procedure

```

---

### *Block Weak Design*

Determining  $d$  from  $t$  is not so simple, we have to pay attention to some constraints: the  $GF(2^x)$ , on which the weak design is based, only works with values of  $t$  that are powers of 2, thus we need to choose larger values of  $t$  than requested from one-bit extractor (and this implies a bigger initial seed  $d$ ), because the one-bit extractor works with arbitrary values of  $t$ . Thus we need to increase  $t$  to the nearest power of 2. Therefore we have to distinguish between  $t$ , that is the value relative to the weak design used to carry out calculations in  $GF(t)$ , and  $t_{req}$ , which is the value required by the bit extractor. This implies necessarily that  $t \geq t_{req}$ .

---

```

1: procedure SWDCOMPUTES $S_i(i, m, t, t_{req})$ 
2:    $c = \lceil \log_2(m) / \log_2(t_{req}) - 1 \rceil$ 
3:    $\text{mask} = (1 \ll \log_2(t)) - 1$ 
4:   for  $j \leq c$  do
5:      $\alpha[j] = (i \wedge (\text{mask} \ll j \cdot \log_2(t))) \gg j \cdot \log_2(t)$ 
6:   end for
7:   for  $a < t_{req}$  do
8:      $b = 0$ 
9:      $Sa = 0$ 
10:    for  $k \leq c$  do
11:       $b \leftarrow b + \alpha[k] \cdot a^k$  ▷ All this operations are computed over  $GF(t)$ 
12:    end for
13:     $Sa = Sa \oplus b$ 
14:     $Sa = Sa \oplus (a \ll \log_2(t))$ 
15:     $S[a] = Sa$ 
16:  end for
17:  return  $S$ 
18: end procedure

```

---

Finite fields of order  $2^m$  are called binary fields or characteristic-two finite fields. In finite fields  $GF(2^m)$  all elements of the field are interpreted as polynomials over the binary field, i.e. polynomials whose coefficients are either 0 or 1. In this field there are  $2^m$  polynomials with degree no more than  $m - 1$ , thus the elements of this field can be viewed as  $m$ -bit strings. Each bit in the bit string corresponds to the coefficient of the polynomial taken at the same position. Additions and subtractions in a finite field are performed by adding or subtracting two of the polynomials of this field together,

and then reducing the result modulo 2, while a multiplication can be done as a multiplication modulo an irreducible polynomial used to define the field. Multiplication of polynomials over the binary field can be implemented as simple bit-shift and XOR. The procedure is the following: take two polynomials written as bit strings; perform the classical multiplication considering the two bit strings as integer numbers; if the degree  $d$  of the resulting polynomial is greater than  $m - 1$ , shift the irreducible polynomial  $l$  bit left, where  $l = d - m$  and then perform bitwise XOR. Repeat the previous point until you get a polynomial of degree  $m - 1$ . The block weak design is based on a basic design whose matrix representation is re-used different times to create the total weak design: once the matrix representation of the basic design has been calculated, it is possible to construct the complete design by placing sub-matrices of the basic design matrix on the diagonal of a larger matrix. If we consider the basic design as a vector of indices instead of a matrix, it is possible to compute the content of  $W_{B,j}$  from the basic row  $W_{B,0}$  by adding  $j \cdot t^2$  to all values of the set  $S$  corresponding to the matrix row.

---

```

1: procedure BWDcompute $S_i(ic, i, m, t, t_{req})$ 
2:    $r' = 2e$ 
3:    $l = \max \left\{ 1, \left\lceil \frac{\log(m-r') - \log(t-r')}{\log(r') - \log(r'-1)} \right\rceil \right\}$ 
4:    $j = i \bmod l$ 
5:    $k_1 = i/l$ ;
6:    $n_0 = (m/r' - 1)$ 
7:    $m_0 = \lceil n_0 \rceil$ 
8:   if  $k_1 \neq ic$  then
9:      $ic = k_1$ 
10:    SWDcompute $S_i(ic, m_0, t, t_{req})$ 
11:    for  $h < t_{req}$  do
12:       $S_c[h] = S[h]$ 
13:    end for
14:  else
15:    for  $h < t_{req}$  do
16:       $S[h] = S_c[h] + j \cdot t^2$ 
17:    end for
18:  end if
19:  return  $S$ 
20: end procedure

```

---

-

## One-Bit extractor

The algorithm to perform polynomial hashing is based on a concatenation of a Reed-Solomon and a Hadamard code as follows:

---

```

1: procedure 1-BIT EXTRACTOR(seed, source,  $n$ ,  $\epsilon$ )
2:    $l = \lceil \log_2(n) + 2 \log_2(2/\epsilon) \rceil$ 
3:    $s = \lceil n/l \rceil$ 
4:    $b = 0$ 
5:   for  $i < n$  do
6:     totalsource[ $i$ ] = source[ $i$ ]
7:   end for
8:   for  $i = n; i < s \cdot l$  do
9:     totalsource[ $i$ ] = 0
10:  end for
11:  for  $i < l$  do
12:     $r[i] = 0$ 
13:  end for
14:  for  $i < s$  do
15:    for  $j < l$  do
16:       $c[i][j] = \text{totalsource}[i \cdot l + j]$ 
17:    end for
18:  end for
19:  for  $i < l$  do ▷ Reed-Solomon step
20:     $\alpha[i] = \text{seed}[i]$ 
21:  end for
22:  for  $j = 1; j \leq s$  do
23:     $a = c[j-1] \cdot \alpha^{j-1}$  ▷ All this operations are computed over  $GF(2^l)$ 
24:    for  $i < l$  do
25:       $r[i] = r[i] \oplus a[i]$ 
26:    end for
27:  end for
28:  for  $i < l$  do ▷ Hadamard step
29:     $b = b \oplus (\text{seed}[i+l] \wedge r[i])$ 
30:  end for
31:  return  $b$ 
32: end procedure

```

---

- [1] N. Nisan and A. Ta-Shma. Extracting randomness: A survey and new constructions. *Journal of Computer and System Sciences*, 58:148–173, 1999.
- [2] R. Shaltiel, *An Introduction to Randomness Extractors, Automata, Languages and Programming*, Lecture Notes in Computer Science, Vol. 6756 (Springer, Berlin, 2011), p. 21.
- [3] Anindya De, Christopher Portmann, Thomas Vidick, and Renato Renner, "Trevisan's extractor in the presence of quantum side information," *SIAM Journal on Computing* 41, 915–940 (2012), arXiv:0912.551
- [4] L. Trevisan, *J. ACM* 48, 2001 (1999).
- [5] A. De, C. Portmann, T. Vidick, and R. Renner, *SIAM J. Comput.* 41, 915 (2012)
- [6] R. Raz, O. Reingold, and S. Vadhan, *J. Comput. Syst. Sci.* 65, 97 (2002).
- [7] X. Ma, F. Xu, H. Xu, X. Tan, B. Qi, and H.-K. Lo, Postprocessing for Quantum Random-Number Generators: Entropy Evaluation and Randomness Extraction, *Phys. Rev. A* 87, 062327 (2013)
- [8] W. Maurer, C. Portmann, and V. B. Scholz, "A modular framework for randomness extraction based on Trevisan's construction," arXiv:1212.0520v1
- [9] Salil Vadhan, "The unified theory of pseudorandomness: guest column," *SIGACT News* 38 (2007).
- [10] Noam Nisan and Avi Wigderson, "Hardness vs randomness," *Journal of Computer and System Sciences* 49, 149–167 (1994).
- [11] Xiongfeng Ma and Xiaoqing Tan, An explicit combinatorial design, Tech. Rep. (2011) eprint, <http://arxiv.org/abs/arXiv:1109.6147> arXiv:1109.61
- [12] Renato Renner, Security of Quantum Key Distribution, Ph.D. thesis, Swiss Federal Institute of Technology Zurich (2005), <http://arxiv.org/abs/quant-ph/0512258> quant-ph/05122